Dynamic micromechanical properties of styrene–butadiene copolymer latex films

J. Richard
Rhône-Poulenc Recherches, Centre de Recherches d'Aubervilliers, Service Application Polymères Dispersés, 52 Rue de la Haie Coq, 93308 Aubervilliers Cedex, France
(Received 4 September 1990; revised 23 October 1990; accepted 23 October 1990)

Polymer films of various gel fractions, obtained by coalescence of styrene–butadiene (SB) copolymer latices, are investigated for their viscoelastic behaviour by dynamic micromechanical spectroscopy. Isochronal temperature dependences of the storage modulus (E'), loss modulus (E'') and loss tangent ($\tan\delta$) are measured in the temperature range -50 to $+130$°C including the glass transition of the polymer films. Then, it is shown that the criteria of applicability for the superposition principle are fulfilled. It follows that master curves for the isothermal frequency dependence of the moduli (E', E'') can be obtained over a wide range of frequency (10^{-7} to 500 rad s^{-1}), with shift factors obeying a law of the Williams–Landel–Ferry type. The key parameters describing the effects of degree of crosslinking and molecular interactions on the viscoelastic behaviour of the films are worked out. They are investigated at different scales (macroscopic, molecular, local) and their dependence upon chain-transfer-agent concentration, which controls the crosslinking process in the system, are determined. Moreover, it is shown that a local parameter, such as the monomeric friction coefficient, can be connected with the glass transition temperature of the SB copolymer film. Finally, the influence of the structure of the films arising from incompletely achieved coalescence of latex particles is discussed.

(Keywords: dynamic mechanical properties; films; copolymer; styrene–butadiene; latex; cross-linking)

INTRODUCTION

Synthetic latices consist of colloidally dispersed polymer particles, which can be prepared by a well controlled emulsion polymerization technique. These aqueous dispersions are commonly used in many applications, such as water-based adhesives, paints, paper coating and textile sizing. Most of the applications require the latex to form a continuous film upon drying and also bind mineral charges within a composite layer. The formation of a film from a latex has been fully studied[1–3]. It results from coalescence of the particles, provided that forces produced during water evaporation are strong enough to overcome both coulombic repulsion forces of the charged particles and particle rigidity[1,2,4]. Further characterization of polymer films obtained in that way is obviously needed, particularly concerning structural and mechanical aspects. A great deal of effort has recently been paid to the structural properties of latex films at the particle size level. For instance, the degree of coalescence of particles and their ordering within the films were carefully investigated by means of well suited techniques, such as small-angle neutron scattering (SANS)[5,6] or transmission electron microscopy (TEM) performed on stained microtomed samples[7]. In contrast, the viscoelastic behaviour of latex films remains a poorly investigated field of research, although mechanical properties should be considered as a powerful non-destructive probe[8,9]. Only a few results have been reported and most of the studies were devoted to either latices obtained in a multistage emulsion polymerization or blends of latex particles[9]. Dynamic micromechanical characterization was used as a probe of the heterogeneous structure of latex films[10,11]. Moreover, it was also shown to be a powerful means for pointing out phase rearrangements upon thermal annealing[12,13]. However, it is to be regretted that these fine studies remain quite qualitative and phenomenological.

The degree of crosslinking of the latex particles and molecular interactions, either within the particles or at particle–particle boundaries, are some of the main features which control the viscoelastic behaviour of latex films. In the present work, we therefore perform a thorough investigation of the effect of particle crosslinking on the dynamic micromechanical properties of latex films. This kind of problem has previously been addressed by Zosel[14]. However, our approach is an attempt to gain a much more quantitative insight into the molecular interactions and local dynamics within the polymer network, through the study of the viscoelastic behaviour of latex films. Crosslinked polymers can exhibit complex and varied network structures related to the nature of the crosslinking process (gelation or vulcanization)[15]. The amount of polymeric material involved in the network, the so-called gel fraction G, is actually one of the main features allowing the description of the random structure of these materials. However, it seems to be of particular interest to obtain characteristic molecular parameters, such as the density of network strands or coupling loci. In our systems, this latter term includes either covalent crosslinking knots or intermolecular interaction loci, such as entanglements for instance[16].

In this paper, we report on micromechanical properties of polymer films obtained from crosslinked polymer latex.

0032-3861/92/030562-10

Table 1 Main features of the synthesized latex particles

Latex	Average composition (wt%)	Average particle size (μm)	CTA conc. (wt%)	Gel fraction (%)
A			2	15
B			1.25	43
C	S:69 B:27	0.18	0.8	69
D			0.4	76
E			0	90

The system chosen consists of a styrene–butadiene (SB) copolymer latex, whose crosslinking process has been controlled during emulsion polymerization by adding a chain transfer agent. One of the main variables of concern in this study is the gel fraction G, which is varied by adjusting the chain-transfer-agent concentration. It will be shown that these experiments enable us to propose a quantitative picture of both the network structure and the local molecular dynamics.

EXPERIMENTAL

Latex preparation

A series of latices having the same composition of styrene and butadiene comonomers were prepared with different chain-transfer-agent concentrations. The corresponding gel fraction values G (see *Table 1*) were measured under mild conditions in chloroform. Dried films were carefully put onto appropriate filters which were dipped in the solvent at room temperature; these filters were then weighed until equilibrium gel fraction values were obtained. The period of time needed for the extraction of the soluble chains was typically about a few days. The emulsion polymerization process used in this work has been extensively described elsewhere[17]: it was carried out in a semi-continuous procedure, where the monomer mixture is added at a rate equal to, or less than, the rate at which it could polymerize[11,17]. The polymerization initiator was ammonium persulphate. We classically used an alkylmercaptan as the chain transfer agent (CTA), with the intention of varying the degree of crosslinking of the polymer. A small amount of an acrylic-type comonomer[6] was also copolymerized in order to improve the stability of the final colloidal dispersions. Conductimetric titration showed that the resulting density of carboxylic acid groups located at the surface of the particles is almost independent of CTA content. Average particle size of all the latices was found to be about 0.18 μm with a narrow width of the corresponding size distribution. The main data concerning the dispersions are given in *Table 1*.

The distribution of branching and crosslinking in this series of copolymers has been thoroughly investigated by Guillot *et al.*[17]. Their theoretical model makes it possible to predict the variations of the gel fraction G *versus* conversion: it shows that, in the present system, for a high CTA content, the G value is likely to increase markedly at the end of conversion, through the coupling of growing free radicals to pendant vinyl groups[17]. Other mechanisms involving transfer to the polymer through allylic hydrogen abstraction, which could give rise to branching, have been found to play a minor role[17]. In the whole process, the CTA content is thought to control the density of effective coupling loci during the crosslinking step described above.

Film formation

Polymer films were obtained by casting the above latices in silicon dishes of well controlled depth, and evaporating water at a temperature of 50°C until homogeneous, transparent, solid films were achieved. Samples were then cut to typical dimensions of about 5×1 cm^2, and they exhibited a constant thickness ranging between 0.7 and 1.6 mm. They were stored under vacuum in a desiccating vessel prior to use.

Dynamic micromechanical analysis (d.m.a.)

The dynamic micromechanical behaviour of the films was investigated using a Rheometrix RDS-LA viscoelastometer equipped with an attachment for temperature control. This apparatus enabled us to measure the storage modulus (E'), the loss modulus (E'') and the loss tangent ($\tan\delta$) over a wide range of temperature (-50 to $+130$°C). The isochronal temperature dependences of E', E'' and $\tan\delta$ were obtained for a frequency of 1 Hz at a constant heating rate of 2°C min^{-1} under a nitrogen atmosphere. The accuracy of the data values was checked by repeating measurements twice in the same temperature range and the reproducibility was found to be satisfactory. Moreover, to obtain more fruitful information, the isothermal frequency dependence was also deduced by sweeping the frequency of the oscillating deformation between 10^{-1} and 500 rad s^{-1}, at different temperatures close to the glass transition temperature. Samples were run at the lowest temperature first, with successive runs at higher temperatures. Finally, the lower-temperature response was checked to ensure that no degradation of the sample had occurred. Recorded spectra were then superimposed by simply shifting them along the frequency axis. Criteria of applicability of the method of reduced variables were fulfilled, as will be shown later. For all the measurements, either isochronal or isothermal, we choose simple extension as the deformation mode. The strain amplitude ε ranged between 5×10^{-4} and 3×10^{-3}. This range was checked to lie in the linear viscoelastic regime, where the moduli are expected to be independent of the deformation amplitude. Tensile deformations provide the same information as shear deformation as long as the incompressibility assumption is not violated. In this case, the tensile modulus E^* is directly related to the shear modulus G^* ($E^* = 3G^*$).

RESULTS AND DISCUSSION

Typical isochronal temperature dependences of E', E'' and $\tan\delta$ recorded under the above conditions for our latex films are plotted in *Figure 1*. These curves classically display three regions where the viscoelastic behaviour of the polymers is well identified: these are the glassy region in the low-temperature range, then the transition zone and finally the rubbery region in the higher-temperature range. In the glassy state, the value of the storage modulus E'_g is high, about 1 GPa, and almost temperature-independent. In the rubbery state, E', whose variations are slow, exhibits a value about three orders of magnitude lower than E'_g. In addition, the occurrence of a more or less pronounced modulus plateau in this region is related to the elasticity of the polymer network, which consists

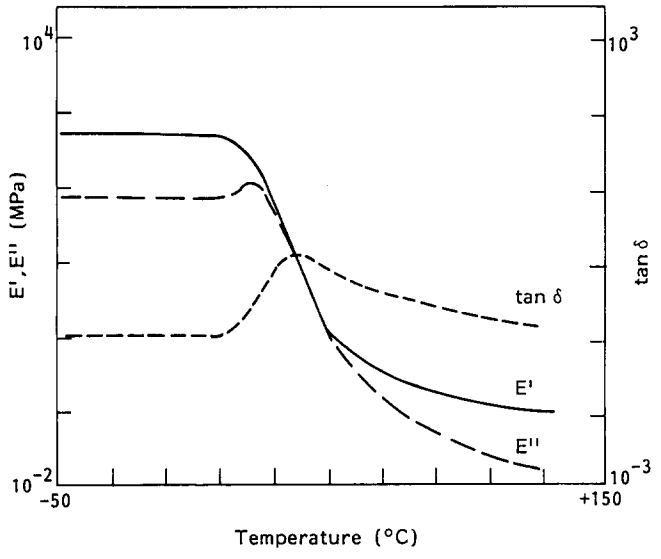

Figure 1 Typical isochronal temperature dependence of the storage modulus (E'), loss modulus (E'') and loss tangent (tan δ) recorded for our latex films. The experimental conditions were the following: strain amplitude $\varepsilon = 10^{-3}$; frequency $f = 1$ Hz; constant heating rate 2°C min^{-1}

Table 2 T_g and T_M values measured for latex films with different CTA concentrations

Latex film	CTA conc. (wt%)	T_g (°C)	T_M (°C)
A	2	23	37
B	1.25	24	37
C	0.8	28	40
D	0.4	36	46
E	0	42	49

of both chemical crosslinks and molecular interaction loci. Besides, it is worth while noticing that E'' and tan δ both pass through a maximum value in the transition zone from glassy to rubbery state. This behaviour is quite consistent with literature data[10,11,18]. Following Misra *et al.*[11] and Zosel[14], we define the glass transition temperature T_g as corresponding to the maximum value of E''. Obviously, this is not the exact definition for T_g, which should involve the discontinuity in the thermal expansion coefficient α[19,20]. However, it enables us to compare the samples from the viewpoint of their mechanical features.

The T_g values measured in that way for our samples are shown in *Table 2*, together with the associated T_M values, which are the temperatures corresponding to the maximum of tan δ. It turns out that T_g markedly increases with increasing crosslinking of the polymer. Moreover, the dependence of T_g upon CTA concentration (*Figure 2*) clearly shows that this effect becomes steady when CTA concentration becomes low, i.e. for a higher and higher density of the polymer network. The above behaviour has already been described for bulk polymer films and theories have been developed so as to relate the shift in T_g to the degree of crosslinking[18,21].

Figure 3 shows the isochronal temperature dependence of the storage modulus E' obtained for films of latex A, C and E, which contain different CTA concentrations. The high-temperature rubber-like behaviour appears to be very sensitive to CTA concentration. This effect is not unexpected, since the CTA content is thought to control the density of the crosslinked network, which is in turn straightforwardly connected with the rubber elastic modulus E'_r[14,16,18–19]. As a matter of fact, the plateau modulus value is found to increase as CTA concentration is progressively decreased.

In order to get a more complete picture of the viscoelastic behaviour of these latex films, the isothermal frequency dependence of E', E'' and tan δ have also been recorded following the procedure given in the experimental section. The empirical principle of time–temperature superposition (or method of reduced

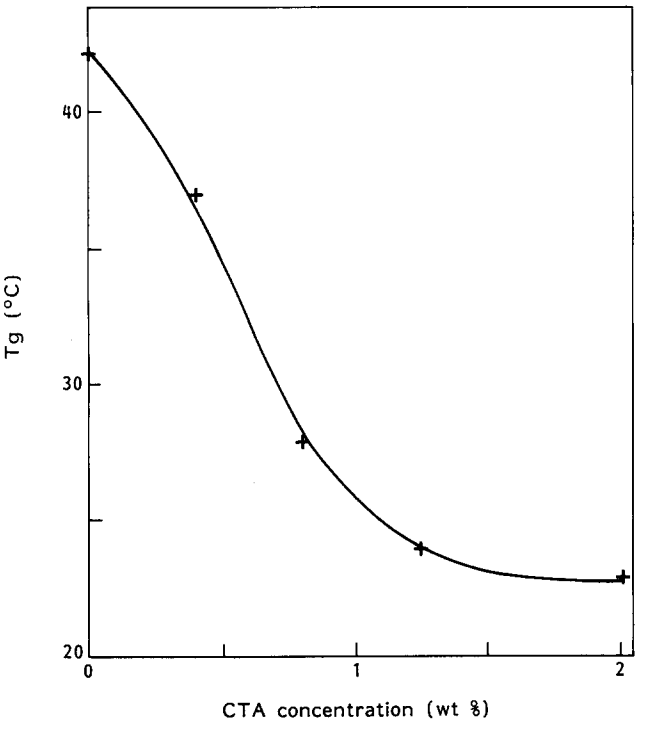

Figure 2 Dependence of the glass transition temperature T_g of the films upon the CTA concentration in the latex. T_g values were determined from the peak in the loss modulus spectrum[11,14]

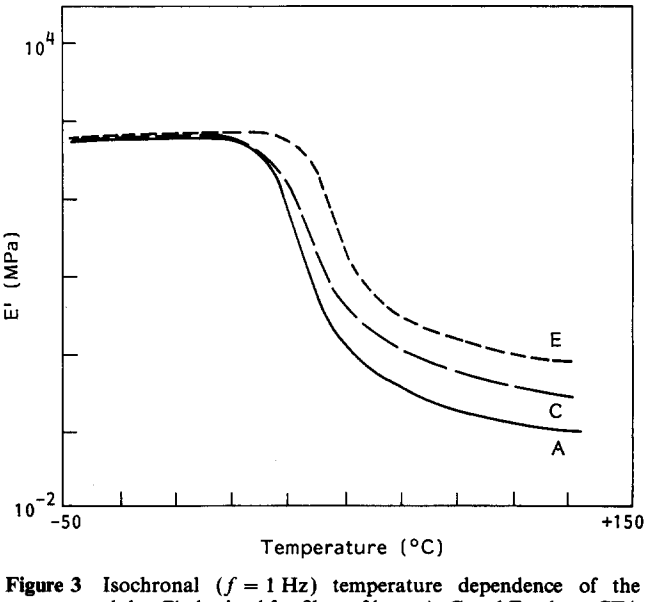

Figure 3 Isochronal ($f = 1$ Hz) temperature dependence of the storage modulus E' obtained for films of latex A, C and E, whose CTA concentrations are 2%, 0.8% and 0% respectively. The high-temperature rubber-like behaviour appears to be very sensitive to CTA content

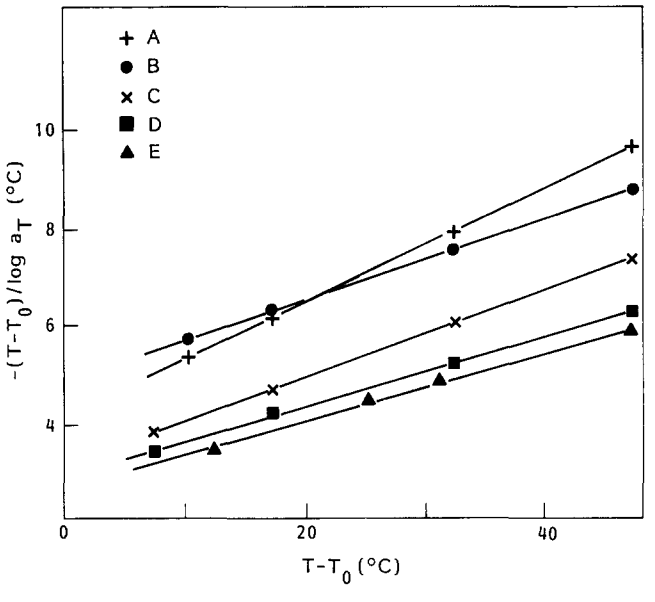

Figure 4 Plots of $-(T - T_0)/\log a_T$ *versus* $T - T_0$ for the whole series of latex films. The observed linear dependence is consistent with a WLF law for the temperature dependence of the frequency shift factor a_T. Values of c_1^0 and c_2^0 can be derived from the slope of the straight lines and their intercept with the vertical axis (*Table 3*)

variables) has been used to derive master curves over a wide range of frequency. This principle states that the complex moduli $E^*(\omega, T)$ at two temperatures are related by a simple scale change:

$$E^*(\omega, T) = b_T E^*(a_T\omega, T_0) \qquad (1)$$

where ω is the deformation frequency, T_0 an arbitrary reference temperature, and b_T and a_T are the modulus scale shift factor and the frequency scale shift factor respectively. These adjustable parameters are functions of temperature, but not frequency[19].

Applicability of reduced variables requires some criteria to be fulfilled. Besides the exact matching of the shapes of adjacent curves, two main prerequisites have been given by Ferry[19], as follows: (a) the same values of a_T must superpose all the viscoelastic functions which are E', E'' and $\tan\delta$ in the present case; (b) the temperature dependence of a_T must have a reasonable form, which can be fitted by the well known WLF expression[22]:

$$\log a_T = -c_1^0(T - T_0)/(c_2^0 + T - T_0) \qquad (2)$$

where c_1^0 and c_2^0 are constants taken at the reference temperature T_0.

For our samples, T_0 was chosen to be close to the glass transition temperature of the polymers, i.e. $T_0 = 28°C$. Modulus scale shift factors b_T were found to be unity within experimental error and will not be discussed here. Furthermore, we checked experimentally that the former criterion (a) was indeed satisfied. Concerning the latter criterion (b), we plotted $-(T - T_0)/\log a_T$ against $T - T_0$ for the whole series of latex films (*Figure 4*). We obtained in this way the linear dependence which is expected for a relationship of the WLF type. The variations of $\log a_T$ *versus* $T - T_0$ for films of latices A, C and E are shown in *Figure 5*. They were obtained by using data at four temperatures between 28 and 75°C. The main feature of these curves is that their shape is quite reminiscent of that described classically for bulk polymers[19]. Moreover they shed light upon the separation of variables resulting from the application of the superposition principle since, starting from a complicated dependence on both temperature and frequency, viscoelastic properties of the films can be expressed as a function of temperature alone. The values of the constants c_1^0 and c_2^0 for a reference temperature $T_0 = 28°C$ were also derived from the plots of *Figure 4* (*Table 3*). They are found to be in the same order of magnitude as constants obtained for bulk polymer samples near their glass transition temperature[19,23,24]. In addition, the ratio c_1^0/c_2^0 ranges about a few degrees only, as predicted by Ferry[19] for a reference temperature close to T_g. Hence all our results appear to be quite satisfactory compared to data reported for bulk polymer samples and therefore enable us to conclude that the superposition principle is obeyed, with the shift factors following an equation of the WLF type.

Typical isothermal master curves obtained for the frequency dependence of the moduli of our latex films are shown in *Figure 6*. To save space, the original data are not given, but they are represented graphically after reduction to $T_0 = 28°C$. The main feature of these spectra is a strong relaxation phenomenon from a glass-like behaviour in the high-frequency range towards a

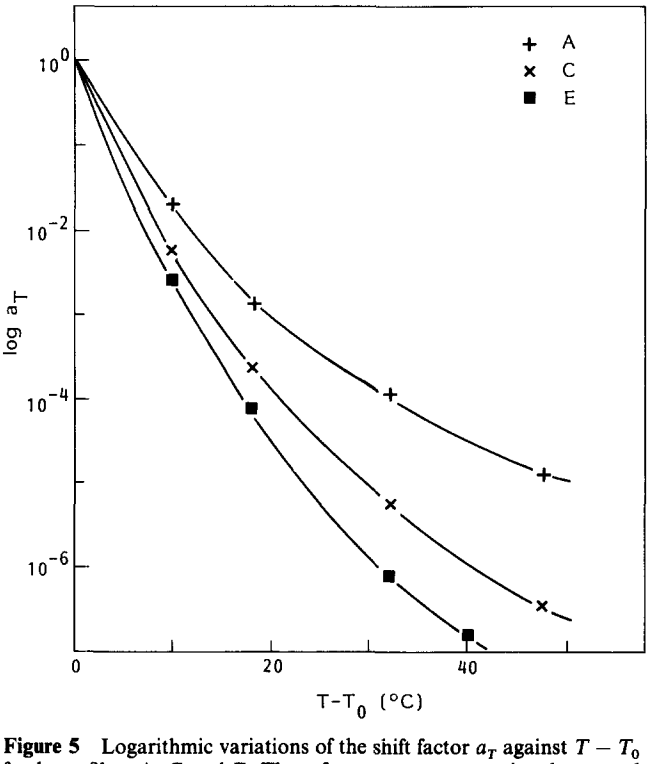

Figure 5 Logarithmic variations of the shift factor a_T against $T - T_0$ for latex films A, C and E. The reference temperature is taken equal to 28°C

Table 3 The c_1^0 and c_2^0 values measured for latex films with different CTA concentrations. The value of the reference temperature T_0 is 28°C. The accuracy of the values of the constants c_1^0 and c_2^0 is estimated to be within 10%

Latex film	CTA conc. (wt%)	c_1^0	c_2^0 (°C)
A	2	8	32
B	1.25	11	53
C	0.8	12	36
D	0.4	14	41
E	0	14	53

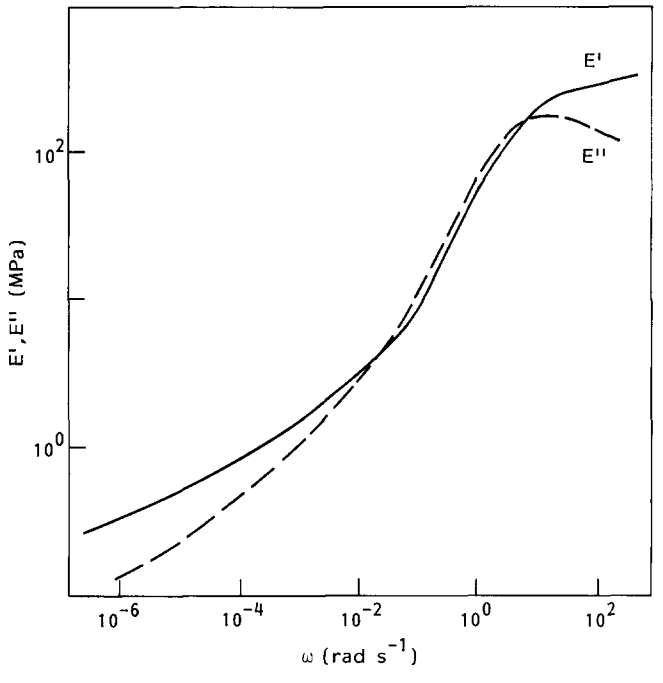

Figure 6 Typical isothermal (log–log) master curves for the frequency dependence of the moduli E' and E'' of latex films. The reference temperature at which the data have been reduced is $T_0 = 28°C$

rubber-like one in the lower-frequency region. The more or less well defined plateau of storage modulus in the latter region is related to the presence of a domain of much slower relaxation due to the presence of a polymer network. Besides, the loss modulus E'' passes through a maximum value in the transition zone, and then falls off in just the same way as the elastic modulus. Another noteworthy detail is the frequency dependence of the moduli within the transition zone. This region always includes a frequency range, at least over a decade, where the values of E' and E'' are almost equal and proportional to the square root of frequency. This behaviour is consistent with the prediction of the Rouse theory applied to concentrated systems[19], from which parameters describing the local monomer dynamics can be derived[19,23]. Finally, logarithmic plots of the dependence of the storage modulus against frequency obtained for the whole series of latex films are gathered in *Figure 7*. The striking differences between the shape of these spectra and their position on the frequency scale will be discussed later.

Coming back now to the d.m.a. investigation of the polymer network features, we first focus on results quoted in *Table 3* and *Figure 5*. Although the value of the constant c_1^0 tends to increase when the CTA content is progressively decreased, no clear correlation can be deduced between the variations of these parameters. However, qualitative arguments can be brought out: according to Ferry[19] and Chee[20], c_1^0 should be inversely proportional to the free-volume fraction (v_0) in the polymer at temperature T_0. Hence, the above result suggests that increasing the density of network strands should result in the decrease of the free volume at a given temperature. This behaviour is not unexpected, insofar as we have shown that the glass transition temperature is strikingly dependent on the CTA content and hence the density of coupling loci. Inspection of the plots in *Figure 5* provides more convincing evidence of the influence of crosslinking and molecular interactions on the viscoelastic behaviour of the films: in fact, the variations of the frequency shift factor a_T *versus* temperature markedly depend on CTA content. This effect is probably due to the fact that a_T is directly connected with the molecular relaxation times and their temperature dependence[19]. Therefore, the above results clearly show that CTA concentration controls the molecular dynamics in these systems. They additionally suggest that molecular relaxation times should vary over a wide range, depending on the CTA concentration in the latex. A more quantitative insight into this point will be given in the next section.

In a second step, we would like to point out that inspection of spectra in *Figure 7* provides more fruitful information. Two effects of the CTA content on the viscoelastic properties of latex films have to be singled out. First of all, with progressively increasing CTA concentration, the location of the transition zone on the frequency scale shifts to higher frequencies, traversing almost four decades of the logarithmic frequency scale. This observation is consistent with the shift in T_g, previously evidenced by plotting the isochronal temperature dependence of the moduli. As proposed by Ferry[19], this displacement obviously reflects a decrease in the relaxation times. More particularly, it points out a strong correlation between the strand size of the network and local molecular motions, even at the monomer level[16,19], and it is susceptible to direct molecular interpretation, as will be shown later. Secondly, the level of E' approached at low frequencies, which should represent the equilibrium modulus of the rubber-like network, appears to fall with increasing CTA content. A high CTA concentration even leads to an almost complete collapse of the modulus in this region. In this limit, the polymer probably begins to enter the terminal zone, where the viscoelastic properties are dominated by the longest

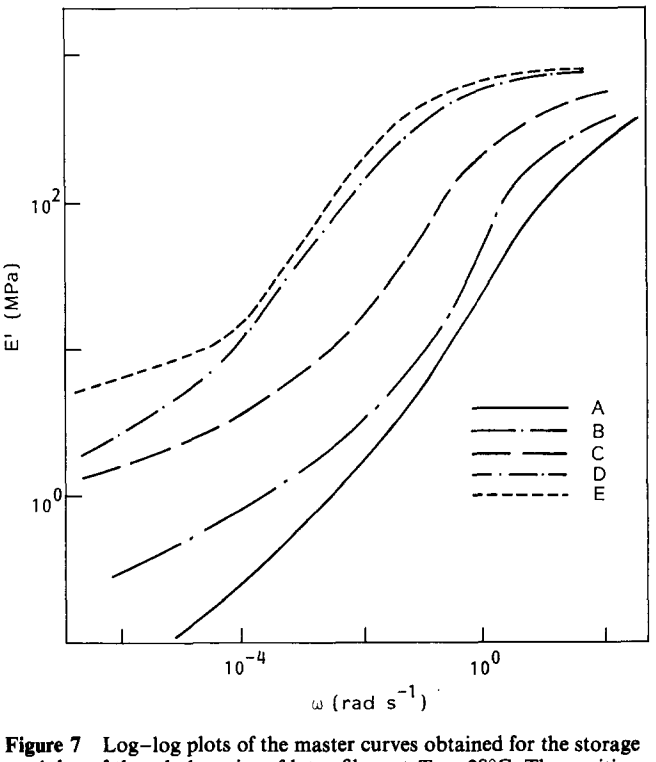

Figure 7 Log–log plots of the master curves obtained for the storage modulus of the whole series of latex films at $T_0 = 28°C$. The position of the transition zone and the value of the rubber-like modulus in the low-frequency region appear to be very sensitive to CTA content

relaxation times[16,19]. It is worth noticing that theory predicts no terminal zone for crosslinked polymers, since the constant equilibrium modulus should persist in the zero-frequency limit. Hence, our results bring out strong additional evidence for the decrease in the density of molecular coupling loci, and particularly covalent crosslinking knots, with increasing CTA content in the polymer latex.

TOWARDS A QUANTITATIVE APPROACH

The aim of this section is to provide quantitative insight into the characteristic parameters of the polymer network and to derive correlations between these features and the CTA content or the corresponding gel fraction G.

A satisfactory description of a polymer network structure can be obtained by deriving the density of elastically effective network strands ν_c (mol cm^{-3}), and then the average molecular weight between coupling loci M_c (g mol^{-1}). As previously discussed, these points arise from either covalent multifunctional links or physical intermolecular interactions. In the latter case, depending on the molecular weight and nature of the comonomers, coupling may be due to intermolecular forces, such as hydrogen bonding between carboxylic comonomers for instance[24], or only due to topological constraints. Then some portions of long chains which are present prior to crosslinking are incorporated, being trapped by the permanent connectedness of the network strands. All these coupling points act as additional restraints and increase the equilibrium rubbery modulus beyond that conferred by chemical crosslinks alone. The relative contributions of chemical crosslinks and molecular interaction loci have been extensively discussed by several authors[19,25,26]. Following Ferry[19], we will assume that the total concentration of effective strands takes into account the additivity of crosslinks and molecular interaction loci to the equilibrium modulus. Further simplifying assumptions are then required. A classical idealization consists of a network of tetrafunctional connectivity, in which four strands of equal length radiate from each coupling point. Dangling ends are not considered and it is assumed that coupling points move in an affine way with deformation of the sample. It can be predicted that the dangling ends and the sol fraction will not contribute to the equilibrium modulus because they cannot store elastic energy at equilibrium. However, they can contribute to the dynamic moduli in a rather complicated way, depending on their length and degree of branching[17,19].

Rouse modes of motion of a molecule whose ends are fixed were investigated by Mooney[27]. He found that the relaxation spectrum includes an additional contribution to the modulus with infinite relaxation time (zero-frequency limit) and magnitude $\nu_c kT$ (k is Boltzmann's constant). In other words, rubber-like response to deformations is obtained because the strands between coupling points can adjust rapidly, whereas entire molecules cannot slip around each other in a finite time to allow flow or completion of stress relaxation. The equilibrium rubber-like storage modulus E'_r can then be related to the moles of elastically effective network strands per volume unit ν_c, as follows:

$$E'_r = 3\nu_c RT \qquad (3)$$

(R is the gas constant). E'_r should theoretically be taken in the low-frequency region of the isothermal master curve, or in the high-temperature zone of the isochronal temperature dependence of the storage modulus. However, in both cases, increasing amounts of relaxation occur throughout the plateau region, making it progressively less well defined. As pointed out by Graessley[16], this is probably due to a broadening of the relaxation-time distribution related to a broadening of molecular-weight distribution. Thus,the curves in *Figure 7* have a sufficient slope to make the selection of E'_r quite uncertain. So, another method has to be used. Then, working with the frequency dependence of the components of the complex compliance J^* ($J^* = 1/E^*$) appears to be a more convenient way to meet the problem. As shown in the frequency dependence of J' and J'' (*Figure 8*), a local maximum clearly appears in the loss component plot (J''), just before the transition zone is entered. This behaviour is typical of polymer networks and was predicted from the suitably modified Rouse theory[27,28]. Moreover, the value of the equilibrium storage modulus E'_r can be deduced from the variations of the loss compliance J''. Besides the sophisticated procedure[19] which consists of integrating over the entire maximum of J'', one can obtain E'_r simply from the peak value J''_m of the loss component. The phenomenological theory developed by Oser and Marvin[29] predicts the following relation:

$$J''_m = A/E'_r \qquad (4)$$

where A is a characteristic constant ranging between 0.24 to 0.42. Following Ferry and coworkers[19,30], we take for A a value which has been shown to give consistent estimates of E'_r for a large number of rubbery polymers, i.e. $A = 0.29$. Then, the set of available relationships which can be used to express the parameters characterizing the network from experimental data E'_r and J''_m can

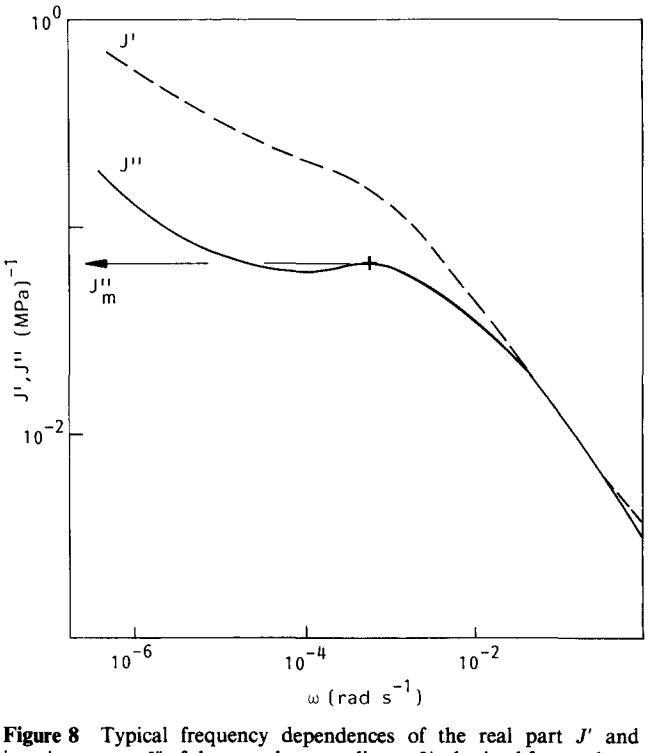

Figure 8 Typical frequency dependences of the real part J' and imaginary part J'' of the complex compliance J^* obtained for our latex films. A maximum J''_m appears in the loss component part (J''), just before the transition zone is entered

Table 4 Values of the density of network strands v_c and the average molecular weight between coupling loci M_c obtained for our latex films, together with the corresponding values of the loss component maximum of the compliance J''_m and the equilibrium rubber-like modulus E'_r

Latex film	J''_m (MPa^{-1})	E'_r (MPa)	v_c ($\mu mol\ cm^{-3}$)	M_c ($g\ mol^{-1}$)
A	2.40	0.12	16	62×10^3
B	0.24	1.2	160	6.2×10^3
C	0.13	2.2	293	3.4×10^3
D	0.10	2.9	386	2.6×10^3
E	0.056	5.2	692	1.4×10^3

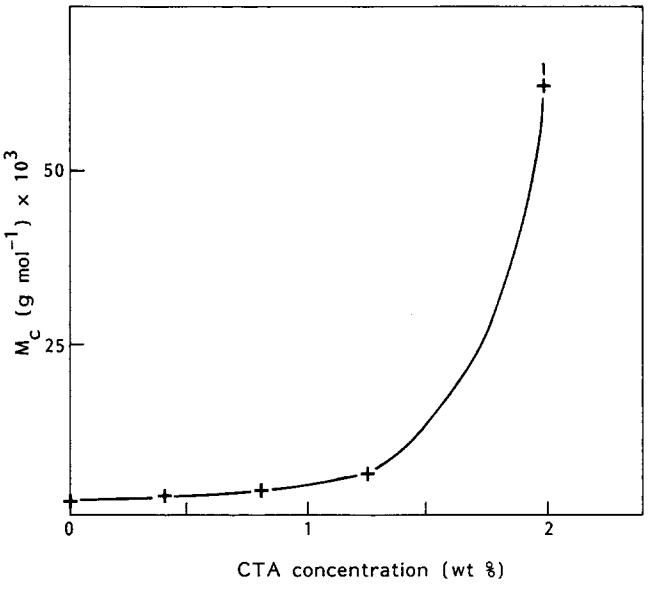

Figure 9 Plot of the variations of the average molecular weight between coupling loci M_c against the CTA concentration

be summarized as follows (ρ is the density of the polymer):

$$J''_m = 0.29/E'_r = 0.29/3v_cRT = 0.29M_c/3\rho RT \quad (5)$$

The values of v_c and M_c obtained in this way for our latex films are gathered in *Table 4*, together with the corresponding values of J''_m and E'_r. As qualitatively predicted from the variations of the shift factor *versus* temperature, the density of network strands varies over a wide spread (about two decades), when CTA content is varied from 0 to 2%. Moreover, the plot of M_c against CTA concentration exhibits a rather greater increase for CTA contents higher than 1.3% (*Figure 9*). This behaviour is not well elucidated. However, it could find its origin in a restriction of the polymer chain length prior to crosslinking when CTA content is higher than 1.3%, resulting in a strong restriction of chain entanglements.

At this point, it seems of particular interest to connect graphically the parameters characterizing the network at the chain level with the main macroscopic feature describing its random structure, i.e. the gel fraction G. For this purpose, the variations of v_c and M_c have been plotted against G (*Figure 10*). Concerning v_c, it turns out that a quasi-linear dependence can be found for G values ranging from 15% to about 70%. Then, v_c increases much more rapidly, as G grows greater than 70%. This behaviour could be attributed to an increasing trapping of chain loops for the highest values of the crosslinking density, which should result in additional network constraints. As discussed previously, these chain loops are latent in the system prior to crosslinking and become permanent features of the network when crosslinking occurs. Thereby, they would increase the equilibrium modulus of the polymer, without necessarily contributing to the gel fraction. The above result suggests that the trapping effect should become considerable, when the crosslinking density becomes higher than a threshold value (ranging about 300 $\mu mol\ cm^{-3}$). Finally, since we previously brought out the shift in the glass transition temperature T_g with varying CTA content and hence the density of network strands v_c, a more quantitative insight into this effect can now be given[18,21]. An equation relating the shift in T_g to the average molecular weight between coupling loci was derived by Di Marzio and Di Benedetto[18]:

$$T_g = T_{g0} + K/M_c \quad (6)$$

where T_{g0} is the glass transition temperature of the uncrosslinked polymer and K a constant. Therefore, we have plotted T_g against $1/M_c$ for the series of latex films (*Figure 11*) and obtained a reasonably linear dependence, as expected from Di Benedetto's calculations. Deviations from the linear plot may be attributed to a composition effect, since the CTA can be considered as a type of copolymerizing unit. Furthermore, the value of K deduced from this plot (about 3.2×10^4 °C $g\ mol^{-1}$) is found to be of the same order of magnitude as that proposed in the literature[18,21]. This result is quite consistent with the fact that the position of the glass transition on the temperature scale is determined by all the molecular interactions within the network.

The second point that we want to work out in a quantitative way concerns the local monomer dynamics. In the above section, we have pointed out that the position of the transition zone on the frequency scale depends on the density of coupling loci. Now, it has long been recognized that this position also reflects local segmental mobility[16,19]. The key molecular parameter

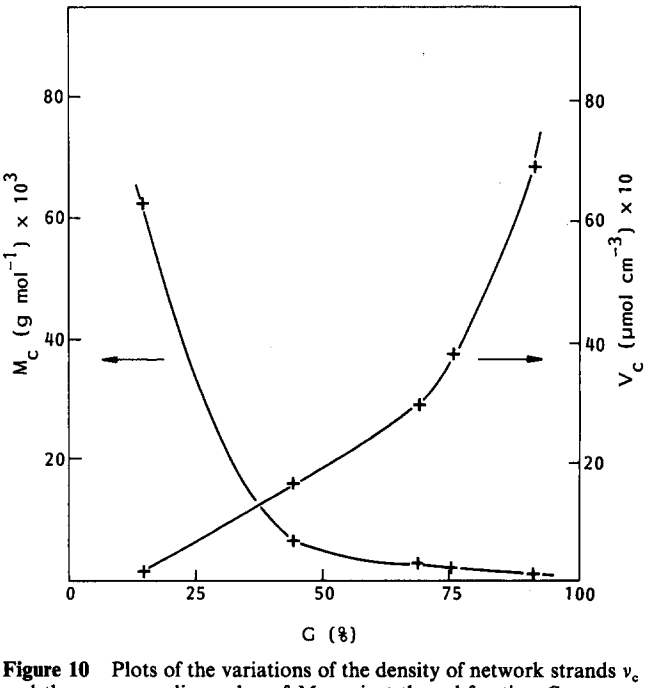

Figure 10 Plots of the variations of the density of network strands v_c and the corresponding value of M_c against the gel fraction G

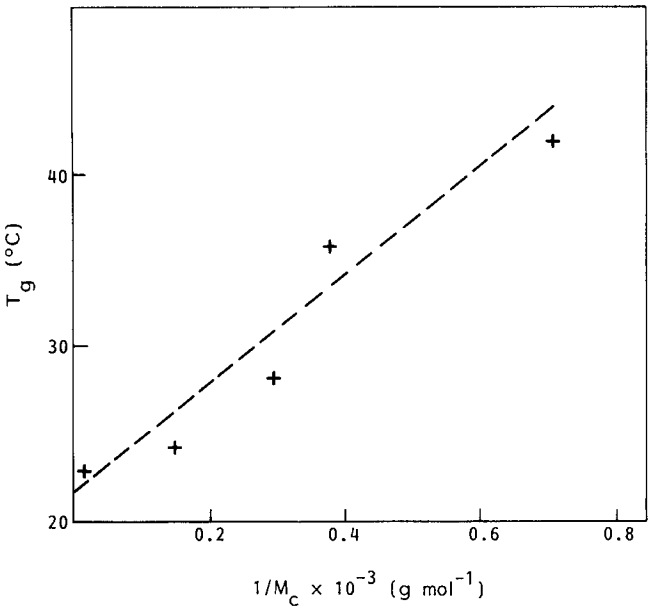

Figure 11 Plot of the variations of the glass transition temperature T_g against $1/M_c$ for the series of latex films. The expected linear dependence is reasonably satisfied[17]

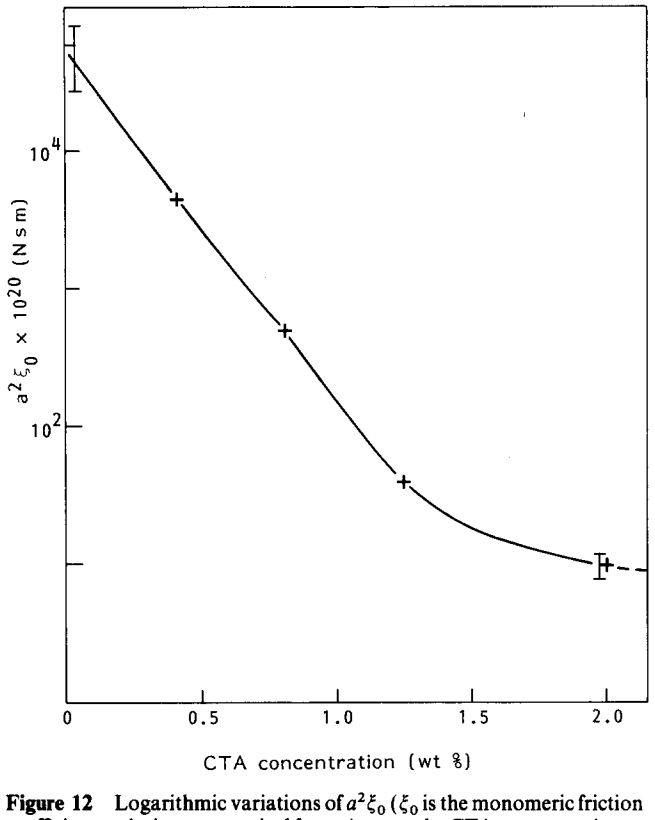

Figure 12 Logarithmic variations of $a^2\xi_0$ (ξ_0 is the monomeric friction coefficient and a is a geometrical factor) *versus* the CTA concentration

which can give a measure of this mobility is the monomeric friction coefficient ξ_0. The significance of ξ_0 is the average frictional force per monomer unit per unit velocity encountered by a submolecule junction as it moves through a medium consisting of other polymer molecules. The values of ξ_0 for the whole series of latex films can be derived from the low-frequency end of the transition zone, where there is a segment of J' and J'' which conforms to the theoretical slope of $-1/2$ on a double logarithmic plot. According to Ferry[19], the following expression can be used to calculate ξ_0 from the master curves of J' and J'' (*Figure 8*):

$$\log J' = \log J'' = -\tfrac{1}{2}\log\omega - \log(a\rho N_0/4M_0) - \tfrac{1}{2}\log(4\xi_0 kT/3) \quad (7)$$

where M_0 is the monomer molecular weight, ρ the density of the polymer, N_0 Avogadro's number and a the root-mean-square end-to-end length per square root of monomer units[19,31]. Specification of a, which depends on local geometric parameters, is somewhat uncertain. So, we have worked directly with $a^2\xi_0$ which can therefore be better determined experimentally than ξ_0 itself. The values of $a^2\xi_0$ have been calculated considering that the monomer molecular weight is equivalent to the weight of a statistical unit of the SB copolymer. As expected from qualitative considerations, it appears that $a^2\xi_0$ is strongly dependent on the CTA content, and *Figure 12* shows more precisely that its logarithmic variations spread over almost four decades. It is worth while noticing that a similar dependence of the local friction coefficient on the density of coupling loci was previously reported by Ferry and coworkers in the case of natural rubber vulcanizates[30]. Furthermore, quite fruitful information concerning local monomer dynamics can be obtained by plotting $a^2\xi_0$ against the average number of monomer units between coupling loci N_c ($N_c = M_c/M_0$) (*Figure 13*). This diagram clearly shows

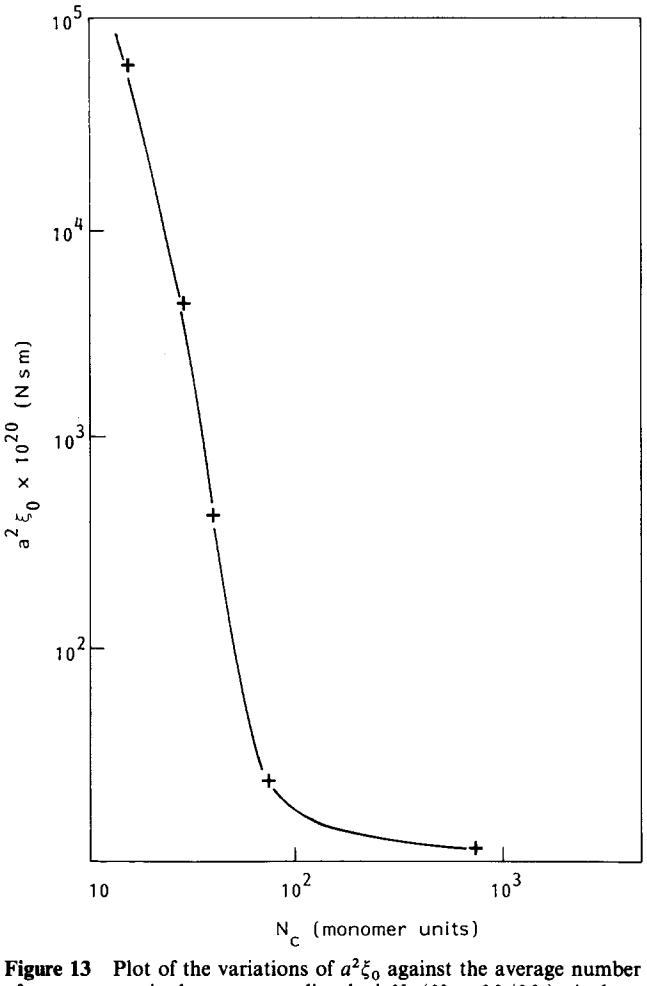

Figure 13 Plot of the variations of $a^2\xi_0$ against the average number of monomer units between coupling loci N_c ($N_c = M_c/M_0$). As long as N_c remains lower than about 10^2 monomer units, the frictional resistance encountered by a chain segment in translatory motions decreases rapidly for increasing values of N_c. Then, it practically does not vary any more for N_c values higher than 10^2 monomer units

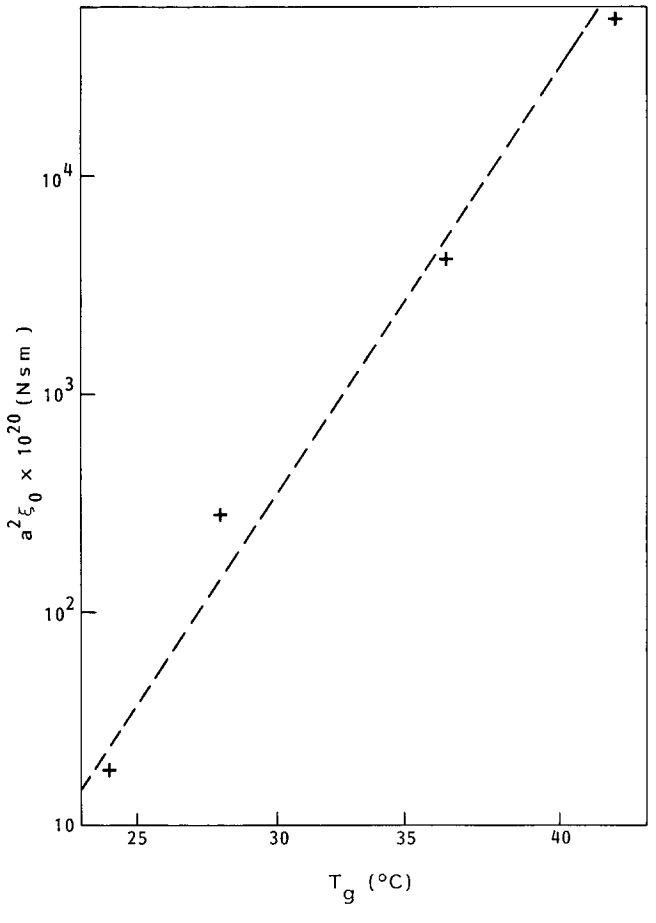

Figure 14 Logarithmic plot of the variations of $a^2\xi_0$ against T_g. When CTA concentration is varied, the dependence is almost linear[30]

that, as long as N_c remains lower than about 10^2 monomer units, the frictional resistance encountered by a chain segment in translatory motions decreases rapidly for increasing values of N_c. In contrast, it practically does not vary any more for N_c values higher than 10^2 monomer units. This behaviour means that the local monomer dynamics is controlled by the tightness of the network, especially when the density of network strands becomes very high, corresponding to a few tens of monomer units between coupling loci. Finally, it appears to be of particular interest to correlate the variations of the monomeric friction coefficient with those of T_g, when CTA concentration is varied. *Figure 14* shows that the logarithmic plot of $a^2\xi_0$ against T_g is almost linear, as has been previously pointed out by Liu *et al.*[31]. This result brings out definite evidence that, at a different scale, each of these data provides a peculiar picture of the same phenomenon, i.e. the strong influence of molecular couplings, either covalent or not, on the local segmental mobility.

CONCLUDING REMARKS

This paper is aimed at providing a refined analysis of micromechanical behaviour of films obtained from aqueous polymer dispersions. As a result, good knowledge of the main features which govern the viscoelastic properties of latex films has indeed been reached by a combination of d.m.a. techniques and investigation methods developed in the field of bulk polymer physics. More particularly, it has been shown that the well known superposition principle can be satisfactorily applied in the case of films obtained from aqueous polymer dispersions, while only a main relaxation phenomenon is concerned. It follows that master curves for the frequency dependence of the moduli can be obtained over a wide range of frequency, with shift factors obeying a law of the WLF type. On a macroscopic scale, our experimental results reveal the key parameters allowing a good description of the effect of degree of crosslinking and molecular interactions upon the viscoelastic behaviour of our films. These data are the shift in the glass transition temperature T_g on varying the density of coupling loci in the polymer network, the position of the transition zone on the frequency scale and, in a more classical way, the value of the equilibrium rubber-like plateau modulus E'_r in the low-frequency region of the master curves. Then, on a molecular scale, the main physical parameters characterizing the network structure have been derived through our quantitative approach. These are the density of network strands ν_c and the corresponding average molecular weight between coupling loci M_c. This step enables us to work out and discuss relationships between these molecular parameters and macroscopically available data, such as T_g or the gel fraction of the polymer G. Then, focusing on a much lower scale, we have finally investigated the local monomer dynamics through the dependence of the monomeric friction coefficient ξ_0 upon the strand size of the network. Hence, the local segmental mobility appears to be directly influenced by the presence of a network, provided its tightness becomes sufficiently high. Conversely, when the network becomes loose, the frictional resistance encountered by a chain segment in translatory motions practically does not vary any more; then, it should only be controlled by the flexibility of the chain[31]. Moreover, it has been shown that this local parameter can be connected with macroscopic data, such as T_g for instance. From a more practical viewpoint, it should be noted that ξ_0 can be readily related to the translatory diffusion coefficient of a chain segment[19], which has been shown to be a useful parameter for describing adhesion between polymers[32].

One of the main limiting assumptions to be fulfilled for obtaining the above pertinent results deals with the homogeneity of the structure of latex films. Thus, when applying polymer network theories to latex films, we have not taken into account the fact that the samples consist of coalesced polymer particles. However, as shown by a TEM analysis performed on stained microtomed latex film E (*Figure 15*), complete coalescence of the particles may not occur depending on the features of the latex, and particularly the crosslinking of the particles[6]. Uncompletely achieved coalescence results in a heterogeneous structure at the particle size level, since interfacial layers, which contain the major part of the hydrophilic material, are still present in the sample. However, it is notable that these heterogeneities appear at a much higher level than the molecular scale. Therefore, we can argue that their contribution to the viscoelastic behaviour of the films as molecular interactions is included in the average molecular features deduced from d.m.a. results, since they do not seem to introduce additional, peculiar, well identified relaxations in the spectra. Obviously, this consideration holds only as long as microstrains are concerned in d.m.a. (i.e. in quasi-equilibrium conditions), and it could not be put forward when investigating

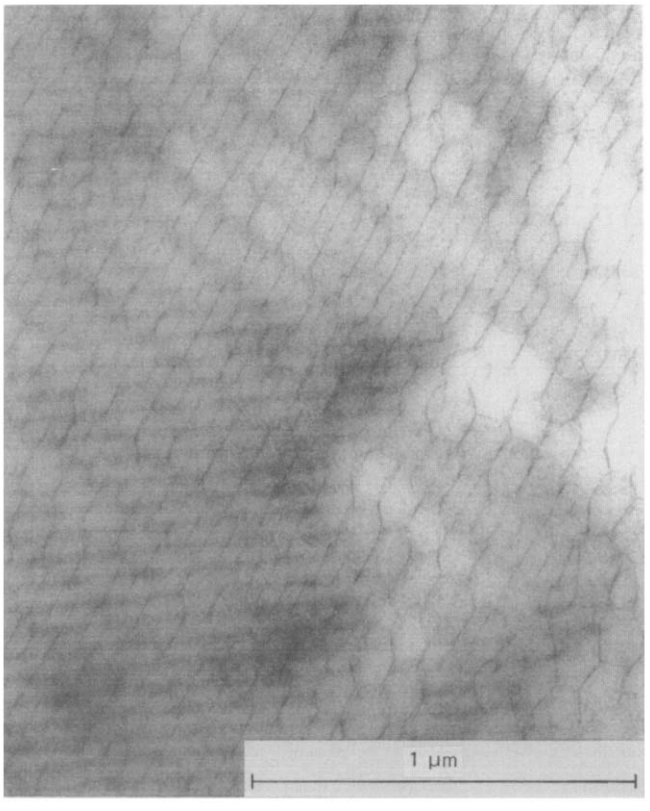

Figure 15 TEM micrograph of stained microtomed latex film E[6]. Incompletely achieved coalescence results in a heterogeneous structure at the particle size level, since interfacial layers are still present in the sample

ultimate stress–strain properties. In some respects, this latter point has recently been shown by Zosel[14]. Nevertheless, from the standpoint of the information gained, one of the most important things to be investigated now is the exact part played by the network of interfacial zones in the viscoelastic behaviour of the films. For this purpose, it will be studied using the same tools as those developed in the present work. In the same way, the effect of ionic groups incorporated in these thin polar regions also needs further investigations through a similar dynamic micromechanical analysis.

ACKNOWLEDGEMENTS

The author gratefully acknowledges Dr J. Maquet (Rhône-Poulenc Recherches) for carrying out the TEM investigation of the latex films and providing him with the photomicrograph included in this work. In the same way, Dr D. Charmot (Rhône-Poulenc Recherches) and F. Desbat (Université de Grenoble I) are gratefully acknowledged for valuable discussions about the crosslinking process in these systems, and for providing us with gel fraction results, respectively.

REFERENCES

1 Brown, G. L. *J. Polym. Sci.* 1956, **22**, 423
2 Vanderhoff, J. W., Tarkowski, H. L., Jenkins, M. C. and Bradford, E. B. *J. Macromol. Sci.* 1966, **1**, 131
3 Lamprecht, J. *Colloid Polym. Sci.* 1980, **258**, 960
4 Sheetz, D. P. *J. Appl. Polym. Sci.* 1965, **9**, 3559
5 Hahn, K., Ley, G., Schuller, H. and Oberthür, R. *Colloid Polym. Sci.* 1986, **264**, 1092; Hahn, K., Ley, G. and Oberthür, R. *Colloid Polym. Sci.* 1988, **266**, 631
6 Joanicot, M., Richard, J., Wong, K., Maquet, J. and Cabane, B. Proc. 64th Colloid Surface Sci. Symp., 1990
7 Distler, D. and Kanig, G. *Colloid Polym. Sci.* 1978, **256**, 1052; Zosel, A., Heckmann, W., Ley, G. and Mächtle, W. Proc. AFTPV Conf., 1985
8 Zosel, A. *Prog. Org. Coat.* 1980, **8**, 47
9 Skrovanek, D. J. and Schoff, C. K. *Prog. Org. Coat.* 1988, **16**, 135
10 Cavaillé, J. Y., Jourdan, C., Kong, X. Z., Perez, J., Pichot, C. and Guillot, J. *Polymer* 1988, **27**, 693
11 Misra, S. C., Pichot, C., El Aasser, M. S. and Vanderhoff, J. W. *J. Polym. Sci., Polym. Chem. Edn* 1983, **21**, 2383
12 Kast, H. *Makromol. Chem., Suppl.* 1985, **10/11**, 447
13 O'Connor, K. M. and Tsaur, S. L. *J. Appl. Polym. Sci.* 1987, **33**, 2007
14 Zosel, A. Proc. AFTPV Conf., 1987
15 Flory, P. 'Principles of Polymer Chemistry', Cornell University Press, Ithaca, New York, 1953
16 Graessley, W. W. *Adv. Polym. Sci.* 1974, **16**, 3
17 Guillot, J. and Charmot, D. Proc. 33rd IUPAC Symp. on Macromolecules, Montreal, 1990; Guillot, J. and Charmot, D. *Polymer* in press
18 Nielsen, L. E. *J. Macromol. Sci.–Rev. Macromol. Chem.* (*C*) 1969, **3** (1), 69
19 Ferry, J. D. 'Viscoelastic Properties of Polymers', Wiley, New York, 1980
20 Chee, K. K. *J. Macromol. Sci.–Phys.* 1988, **27** (4), 305
21 Di Marzio, E. A. *J. Res. Nat. Bur. Stand.* (*A*) 1964, **68**, 611
22 Williams, M. L., Landel, R. F. and Ferry, J. D. *J. Am. Chem. Soc.* 1955, **77**, 3701
23 Sanders, J. F., Ferry, J. D. and Valentine, R. H. *J. Polym. Sci.* (*A-2*) 1968, **6**, 967
24 Navratil, M. and Eisenberg, A. *Macromolecules* 1974, **7**, 84
25 Blanchard, A. F. and Wootton, P. M. *J. Polym. Sci.* 1959, **34**, 627
26 Pearson, D. S. and Graessley, W. W. *Macromolecules* 1978, **11**, 528
27 Mooney, M. *J. Polym. Sci.* 1959, **34**, 599
28 Chompff, A. J. and Duiser, J. A. *J. Chem. Phys.* 1966, **45**, 1505
29 Marvin, R. S. and Oser, H. *J. Res. Nat. Bur. Stand.* (*B*) 1962, **66**, 171; Oser, H. and Marvin, R. S. *J. Res. Nat. Bur. Stand.* (*B*) 1963, **67**, 87
30 Stratton, R. A. and Ferry, J. D. *J. Phys. Chem.* 1963, **67**, 2781
31 Liu, W., Yang, Y. and He, T. *Polymer* 1988, **29**, 1789
32 de Gennes, P. G. *C.R. Acad. Sci. Paris* 1989, **308** (II), 13